

Strong coupling of optical nanoantennas and atomic systems

K. Słowik,¹ R. Filter,¹ J. Straubel,¹ C. Rockstuhl,¹ and F. Lederer¹

¹*Institute of Condensed Matter Theory and Solid State Optics,
Abbe Center of Photonics, Friedrich-Schiller-Universität Jena, D-07743 Jena, Germany*

An optical nanoantenna and adjacent atomic systems are strongly coupled when an excitation is repeatedly exchanged between these subsystems prior to its eventual dissipation into the environment. It remains challenging to reach the strong coupling regime but it is equally rewarding. Once being achieved, promising applications as signal processing at the nanoscale and at the single photon level would come immediately into reach. Here, we study a hybrid configuration from different perspectives that consists of two identical atomic systems, described in a two-level approximation, that are strongly coupled to an optical nanoantenna. First, we investigate when this hybrid system requires a fully quantum description. Second, a design for a nanoantenna is presented that enables indeed the strong coupling regime. Besides a vivid time evolution, the strong coupling is documented in experimentally accessible quantities, such as the extinction spectra. The latter are shown to be strongly modified if the hybrid system is weakly driven and operates at the quantum level. We find that the extinction spectra depend sensitively on the number of atomic systems coupled to the nanoantenna. It therefore holds promise to eventually perceive sensing devices that operate at the single-molecule level.

PACS numbers: 81.16.Ta, 73.21.-b, 78.90.+t, 71.70.Gm,

I. INTRODUCTION

Metallic optical antennas have proven perfect in tailoring light-matter interactions at the nanoscale. They allow to change the spontaneous emission rates of adjacent atomic systems or their radiation properties drastically, see e.g. Refs. [1–4]. Even though the modified light-matter interaction manifests in a multitude of phenomena, they are eventually promoted by the same underlying principle, that metallic optical nanoantennas can support strongly localized surface plasmon polaritons. This is at the heart of all the observations and entails that their coupling to far-field radiation and quantum systems can be engineered on purpose [5, 6].

Recent advances in nanotechnology made it eventually feasible to fabricate nanoantennas with precision down to the atomic scale [7]. This implies that a precise placement of systems such as quantum dots, molecules, or atoms, close to a carefully designed nanoantenna, is possible. It has been already shown that in such situations remarkable new phenomena can be expected where the huge enhancement of dipole-forbidden transitions in the gap of a dimer nanoantenna may serve as a representative example [8, 9]. This tremendous spatial localization of the plasmonic mode enables a strong coupling of quantum systems to nanoantennas. The regime of strong coupling is characterized by a transition from irreversible spontaneous emission and nonradiative damping processes to a reversible energy exchange between nanoantenna and atomic system. Such a behavior has been reported for cavities operating in the infrared and visible spectral domain [10, 11]. To achieve strong coupling is of paramount importance to enable applications for deterministic quantum computation and for high-

power emission into predefined directions of nonclassical light.

In our contribution we want to go one step further and consider two atoms strongly coupled to a nanoantenna rather than a single, isolated one. The aim is to demonstrate that in this case the strong coupling effects are more pronounced. Here, one purpose of the nanoantenna is to mediate a strong interaction between both atoms. Moreover, the structure is highly interesting since it promises to observe a much larger splitting of the energy levels of the hybrid system when compared to that of bare atoms isolated from the nanoantenna. Perspective, this may suggest an alternative route towards artificial atoms with engineered energy levels. Furthermore, the properties of the hybrid system are shown to sensitively depend on the number of atoms or molecules involved, paving the way for ultra-sensitive devices operating on the single molecule level.

Moreover, besides being of importance from an applied perspective, the setup is essential for basic science since it constitutes a system with a rich dynamics that can be operated in different regimes; where each regime requires a well adapted approach to fully grasp its properties. Specifically, the nanoantennas themselves may be described at different levels of approximation. The most direct approach is to consider the nanoantenna as a passive system which can significantly influence the atoms' dynamics whereas it remains unaffected. If such approximation holds, the nanoantenna is treated as a classical harmonic oscillator as frequently done in the literature [12, 13]. This simplifies the treatment considerably but prevents the observation of quantum effects associated with the nanoantenna. On the contrary, one may account for the full dynamics of the electrons inside the nanoantenna. Such an exhaustive treatment is required if the

atoms are placed only a few angstroms off the nanoantenna such that electron-spill-out and quantum tunneling effects become relevant [14, 15]. Nonetheless, these effects have not to be considered in most experimentally accessible situations.

In-between, however, lies a regime where the nanoantenna can be considered as a harmonic oscillator but which requires a proper quantization [16–20]. The approach permits the description of the rich quantum behavior of the hybrid system. It is especially useful to study effects at the low power level where only a few photons are involved. However, it is *a priori* not clear whether such elaborated approach is necessary or whether the semiclassical treatment is already sufficient.

Therefore, at first we will develop both a semiclassical and a full quantum theory for the problem where an atom described in a two-level approximation is coupled to an optical nanoantenna. We will compare the results of both approaches in Section III and will devise unambiguous criteria that can be used to decide, on the base of experimentally accessible quantities, which of the two approaches is necessary. Second, we will explicitly discuss in Section IV the design of a nanoantenna that reaches the strong coupling regime. After that, we study in Section V the impact of the strong coupling on the extinction spectra of a hybrid system where two atoms are coupled to the optical nanoantenna. We find that the presence of the atoms hugely influences both absorption and scattering properties of the hybrid system. After concluding on our findings we provide in elaborated appendices details of our calculations and results that support our conclusions from the main manuscript. In App. A the equations of motion for the semiclassical formulation are derived. Appendix B details our method to calculate the coupling constants of the nanoantenna to the atoms and to the driving field from numerical simulations. Also, the estimation for the radiative and nonradiative decay rates of the nanoantenna is given. In App. C, the eigenstates and -energies in the framework of the full quantum approach are depicted in detail.

II. MODEL

We consider two identical two-level systems. We refer to them as *atoms*, but they could equally describe molecules, quantum dots, NV-centres in diamond, etc.[21] The two-level-systems shall be symmetrically placed next to a mirror-symmetric nanoantenna that is excited with a driving field propagating along the symmetry axis. Schematically, the situation is shown in Fig. 1. It is worth mentioning that this high symmetry configuration is only chosen with the intention to preserve some simplicity in our treatment. It constitutes by no means any limitation.

As discussed above, the theoretical description of such

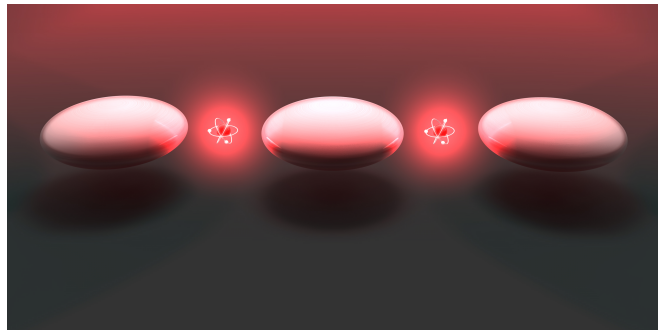


Fig. 1: A general scheme of the considered hybrid system. A nanoantenna is strongly coupled to two atoms and excited by an external driving field.

a system may be performed in several approximations. In subsection II A we consider a fully quantum model including a quantum description of the nanoantenna itself. Such an approach requires in practice a considerable numerical effort, unless the excitation field is rather weak and the total system remains approximately at the single excitation level. A great simplification and limitation of numerical effort is provided by a mean-field approximation, where the electromagnetic field can be described classically. Such a semiclassical treatment will be given in subsection II B. Both models will be compared in the following section.

A. Fully quantum approach

In the fully quantum approach, we regard the nanoantenna as a single mode quantum harmonic oscillator. The Hamiltonian in the rotating frame takes then the following form within the rotating wave approximation [22]:

$$H = \frac{\hbar \Delta\omega_0}{2} \sum_{j=1}^{N_{\text{tIs}}} (\sigma_z^{(j)} + \mathbb{1}) + \hbar\Delta\omega_{\text{na}} a^\dagger a \quad (1)$$

$$- \hbar\kappa \sum_{j=1}^{N_{\text{tIs}}} (\sigma_+^{(j)} a + a^\dagger \sigma_-^{(j)}) - \hbar\Omega (a + a^\dagger),$$

with $\Delta\omega_0 = \omega_0 - \omega_{\text{dr}}$, $\Delta\omega_{\text{na}} = \omega_{\text{na}} - \omega_{\text{dr}}$. Here, $N_{\text{tIs}} = 2$ is the number of identical atoms, and ω_0 corresponds to their transition frequency. The operators $\sigma_z^{(j)} = |e^{(j)}\rangle\langle e^{(j)}| - |g^{(j)}\rangle\langle g^{(j)}|$ represent the population inversion in the j^{th} two-level system, and $\sigma_+^{(j)} = |e^{(j)}\rangle\langle g^{(j)}|$ and $\sigma_-^{(j)} = \sigma_+^{(j)\dagger}$ are the corresponding creation and annihilation operators of atomic excitation. As usual, $\{|e^{(j)}\rangle$ and $|g^{(j)}\rangle\}$ denote the excited and ground state of the j^{th} two-level system.

The nanoantenna is coherently driven by an external laser beam, assumed to be monochromatic at frequency ω_{dr} . Its intensity is related to the Rabi frequency Ω ,

which is here taken real for simplicity. The coupling constant of an atom and the nanoantenna is given by κ , identical for both atoms because of their symmetric placement. Note that κ can be assumed constant, if the transition frequency of the atoms is close to the broad resonance frequency of the nanoantenna, ω_{na} . We neglect the free-space interaction of the atoms, i.e. the dipole-dipole interaction in the absence of the nanoantenna, as it is considerably weaker than the interaction of the atoms due to the nanoantenna. We also neglect the direct coupling of the driving field to the atoms, as, again, it is much weaker than the nanoantenna's scattered field at the position of the atoms.

The dynamics of the hybrid system is described by the Lindblad-Kossakowski equation [22]:

$$i\hbar\dot{\rho} = [H, \rho] + i\mathcal{L}_{\text{na}}(\rho) + i\mathcal{L}_{\text{tls}}(\rho), \quad (2)$$

where ρ is the state density operator of the hybrid system and $\mathcal{L}_{\text{na},\text{tls}}(\rho)$ are Lindblad operators responsible for losses in the nanoantenna and the atoms, respectively, given by

$$\mathcal{L}_{\text{na}}(\rho) = -\hbar\Gamma(a^\dagger a\rho + \rho a^\dagger a - 2a\rho a^\dagger), \quad (3)$$

$$\begin{aligned} \mathcal{L}_{\text{tls}}(\rho) = & -\frac{1}{2}\hbar\Gamma_{\text{fs}}\sum_{j=1}^{N_{\text{tls}}}\left(\sigma_+^{(j)}\sigma_-^{(j)}\rho + \rho\sigma_+^{(j)}\sigma_-^{(j)}\right. \\ & \left.- 2\sigma_-^{(j)}\rho\sigma_+^{(j)}\right) \\ & -\hbar\Gamma_{\text{d}}\sum_{j=1}^{N_{\text{tls}}}\left(\sigma_+^{(j)}\sigma_-^{(j)}\rho + \rho\sigma_+^{(j)}\sigma_-^{(j)}\right. \\ & \left.- 2\sigma_+^{(j)}\sigma_-^{(j)}\rho\sigma_+^{(j)}\sigma_-^{(j)}\right) \end{aligned} \quad (4)$$

In the above expressions $\Gamma = \Gamma_{\text{r}} + \Gamma_{\text{nr}}$ describes radiative and nonradiative losses by the nanoantenna. The free-space spontaneous emission rate of a single two-level system is given by Γ_{fs} , whereas Γ_{d} is the rate of pure dephasing. An example of the latter would be the interactions with phonons in quantum dots that affect the coherence but not the population distribution [23]. Typically, the radiative and nonradiative losses in the metallic nanoparticle are much stronger than all the losses in the atoms.

B. Semiclassical approach

In the preceding subsection we have formally introduced a fully quantum description of the atoms coupled to a nanoantenna. Now the same physical situation will be considered but the description of the nanoantenna will be approximated by a classical equation of motion. The state of the atomic system may then be described by its density operator which we denote as ρ^{sc} . Its evolution follows the Lindblad-Kossakowski equation

$$i\hbar\dot{\rho}^{\text{sc}} = [H^{\text{sc}}, \rho^{\text{sc}}] + i\mathcal{L}_{\text{tls}}(\rho^{\text{sc}}), \quad (5)$$

with the semiclassical Hamiltonian [22]

$$\begin{aligned} H^{\text{sc}} = & \frac{\hbar\Delta\omega_0}{2}\sum_{j=1}^{N_{\text{tls}}}\left(\sigma_z^{(j)} + \mathbb{1}\right) \\ & -\hbar\kappa\sum_{j=1}^{N_{\text{tls}}}\left[\sigma_+^{(j)}\alpha(t) + \alpha^*(t)\sigma_-^{(j)}\right]. \end{aligned} \quad (6)$$

To have an analogy to the fully quantum Hamiltonian H , we denote the Rabi frequency of the scattered field by $\kappa\alpha(t)$, with the classical dimensionless amplitude $\alpha(t) \in \mathbb{C}$.

The time-dependent dipole moment of each atom is naturally an electrodynamic source. Thus, the overall field is a superposition of contributions from the atoms and the nanoantenna. Usually the field generated by the j^{th} atom is expressed by its mean transition dipole moment, $\mathbf{E}(\mathbf{r}, t) \propto \langle \mathbf{d}^{(j)} \rangle = \mathbf{d}_{\text{ge}}^{(j)}\rho_{\text{eg}}^{\text{sc}(j)}$ [12], where $\rho_{\text{mn}}^{\text{sc}(j)} = \rho_{\text{nm}}^{\text{sc}(j)*} = \langle m|\rho^{\text{sc}(j)}|n \rangle$ is an element of the reduced density matrix of the j^{th} atom, and the asterisk stands for the complex-conjugate. As derived in App. A, the evolution equation of the field in the slowly-varying envelope approximation $|\dot{\alpha}| \ll |\alpha\omega_{\text{dr}}|$ and for $\Gamma \ll \omega_{\text{dr}}$ is given by

$$\begin{aligned} \dot{\alpha}(t) = & -(\Gamma + i\Delta\omega_{\text{na}})\alpha(t) \\ & + i\left[\kappa\sum_j \rho_{\text{eg}}^{\text{sc}(j)}(t) + \Omega\right]. \end{aligned} \quad (7)$$

Such a description is an approximation which turns out to be valid just for very weak excitations as we will show in the following section.

III. COMPARISON OF SEMICLASSICAL AND FULLY QUANTUM APPROACH

One of the main issues addressed in this paper concerns the identification of conditions where the semiclassical and the fully quantum approaches are equivalent. To find the answer, we will consider the simplest scenario where a single atom is coupled to the nanoantenna at first. We will directly compare the evolution equations of the atomic operators in the fully quantum approach, obtained in the Heisenberg picture, with the corresponding evolution equations of the atomic density matrix and of the field amplitude in the semiclassical approach. A limit will be identified where both approaches agree to a good approximation. An interpretation in terms of correlation functions will also be provided.

As we will show, the very source of discrepancy between both approaches is the interaction term proportional to κ , which we will now focus on. For this reason we consider for a while a simplified lossless case, and also set $\Omega = 0$, but assume that excitation is initially present

in the coupled system. For instance, the atom is initially excited and/or photons are present in the field of the nanoantenna.

Directly from the Heisenberg equation $\dot{A} = -i/\hbar[A, H]$ we obtain the evolution of the field annihilation operator in the rotating frame in the fully quantum picture:

$$\dot{a}(t) = -i\Delta\omega_{\text{na}}a(t) + i\kappa\sigma_-(t), \quad (8)$$

and of the atomic operators:

$$\dot{\sigma}_z(t) = 2i\kappa [\sigma_+(t)a(t) - a^\dagger(t)\sigma_-(t)], \quad (9)$$

$$\dot{\sigma}_-(t) = -i\Delta\omega_0\sigma_-(t) - i\kappa\sigma_z(t)a(t). \quad (10)$$

The annihilation operator equation can be formally integrated to give

$$a(t) = a(0)e^{-i\Delta\omega_{\text{na}}t} + i\int_0^t \kappa\sigma_-(t')e^{-i\Delta\omega_{\text{na}}(t-t')}dt'. \quad (11)$$

Inserting the latter into equations (9-10) leads to the following evolution equations for the mean values:

$$\begin{aligned} \langle \dot{\sigma}_z(t) \rangle &= 2i\kappa [\langle \sigma_+(t)a(0) \rangle e^{-i\Delta\omega_{\text{na}}t} - \text{c.c.}] \\ &\quad - 2\kappa^2 \int_0^t \langle \sigma_+(t)\sigma_-(t') \rangle e^{-i\Delta\omega_{\text{na}}(t-t')} dt' \\ &\quad - 2\kappa^2 \int_0^t \langle \sigma_+(t')\sigma_-(t) \rangle e^{i\Delta\omega_{\text{na}}(t-t')} dt' \\ \langle \dot{\sigma}_-(t) \rangle &= -i\Delta\omega_0\langle \sigma_-(t) \rangle \\ &\quad - i\kappa\langle \sigma_z(t)a(0) \rangle e^{-i\Delta\omega_{\text{na}}t} \\ &\quad + \kappa^2 \int_0^t \langle \sigma_z(t)\sigma_-(t') \rangle e^{-i\Delta\omega_{\text{na}}(t-t')} dt', \end{aligned} \quad (12)$$

where c.c. stands for the complex-conjugate. We consider here the evolution of mean values of the atomic operators because it can be directly compared with the evolution of the corresponding elements of the density matrix, i.e. $\langle \sigma_z(t) \rangle = \rho_{ee}^{\text{sc}}(t) - \rho_{gg}^{\text{sc}}(t)$, $\langle \sigma_-(t) \rangle = \rho_{eg}^{\text{sc}}(t)$.

Similarly, in the semiclassical description, we integrate equation (7) with Γ and Ω set to zero. Next, we insert it into the Lindblad-Kossakowski equation (5) with $\Omega = 0$ and $\Gamma_{\text{fs}} = \Gamma_{\text{d}} = 0$, to arrive at:

$$\begin{aligned} \dot{\rho}_{ee}^{\text{sc}} - \dot{\rho}_{gg}^{\text{sc}} &= 2i\kappa [\rho_{ge}^{\text{sc}}(t)\alpha(t) - \alpha^*(t)\rho_{eg}^{\text{sc}}(t)] \\ &= 2i\kappa [\rho_{ge}^{\text{sc}}(t)\alpha(0)e^{-i\Delta\omega_{\text{na}}t} - \text{c.c.}] \\ &\quad - 2\kappa^2 \int_0^t \rho_{ge}^{\text{sc}}(t)\rho_{eg}^{\text{sc}}(t')e^{-i\Delta\omega_{\text{na}}(t-t')} dt' \\ &\quad - 2\kappa^2 \int_0^t \rho_{ge}^{\text{sc}}(t')\rho_{eg}^{\text{sc}}(t)e^{i\Delta\omega_{\text{na}}(t-t')} dt' \\ \dot{\rho}_{eg}^{\text{sc}} &= -i\Delta\omega_0\rho_{eg}^{\text{sc}} - i\kappa\alpha(t) [\rho_{ee}^{\text{sc}}(t) - \rho_{gg}^{\text{sc}}(t)] \\ &= -i\Delta\omega_0\rho_{eg}^{\text{sc}} \\ &\quad - i\kappa [\rho_{ee}^{\text{sc}}(t) - \rho_{gg}^{\text{sc}}(t)]\alpha(0)e^{-i\Delta\omega_{\text{na}}t} \\ &\quad + \kappa^2 \int_0^t [\rho_{ee}^{\text{sc}}(t) - \rho_{gg}^{\text{sc}}(t)]\rho_{eg}^{\text{sc}}(t') \times \\ &\quad \times e^{-i\Delta\omega_{\text{na}}(t-t')} dt'. \end{aligned} \quad (13)$$

Now by directly comparing the equations obtained in both descriptions we note that the semiclassical approach leads to nonlinear terms of the type $\rho_{ij}^{\text{sc}}(t)\rho_{kl}^{\text{sc}}(t')$ or, equivalently, $\langle \sigma_p(t) \rangle \langle \sigma_q(t') \rangle$, with $i, j, k, l = e, g$ and $p, q = z, +, -$. On the other hand, from the analysis of the Heisenberg equations of motion, i.e. without the mean field approximation, we can see that terms such as $\langle \sigma_p(t)\sigma_q(t') \rangle$ appear in the equations of motion instead [24].

Both results are only equivalent if the atomic operators are not correlated, i.e. if $\langle \sigma_p(t)\sigma_q(t') \rangle \approx \langle \sigma_p(t) \rangle \langle \sigma_q(t') \rangle$. A similar problem has been investigated in Ref. [25], where the authors use a harmonic oscillator model for a two-level system and demonstrate that the condition of uncorrelated system operators is fulfilled for a harmonic oscillator initially in its ground state. A harmonic oscillator is indeed a good model of a two-level system if its first excited state occupation probability is small, and the doubly and higher excited states are not relevant.

Likewise, a two-level system is a good model for a harmonic oscillator if the system is approximately in its ground state. The bosonic commutation rule can then be recovered for the annihilation and creation operators $[\sigma_-, \sigma_+] = -\sigma_z \approx 1$ and one may apply the result of Ref. [25] to the case of a two-level system. Moreover, only in such case the two-level system is a source of coherent light, which can be accurately described by the semiclassical approximation. Only if the condition of uncorrelated system operators holds true, i.e. the two-level system has to stay approximately in its ground state throughout the entire evolution, the mean field approximation, and so the semiclassical approach, are valid [17]. Note that the applicability of this restriction does not depend on the coupling strength. Furthermore, our condition holds for problems beyond the coupling of two-level systems to nanoantennas considered here, namely in general for any case where atomic systems interact with light.

For calculations it is often crucial to find a strict criterion when the semiclassical approximation can be used. Such a criterion can be found by deriving the steady-state solution of equations (14), where the driving field or loss rates are no longer assumed to be zero. The assumption that must be fulfilled for the semiclassical approximation to be valid is that the excited state occupation of either atomic system is small, i.e. $1 \approx \rho_{gg}^{\text{sc}} \gg \rho_{ee}^{\text{sc}}$. Then, we find

$$\begin{aligned} \rho_{ee}^{\text{sc}} &\approx \frac{2\Gamma_{\text{dec}}\kappa^2\Omega^2}{\Gamma_{\text{fs}}D} \ll 1, \\ D &= (\Gamma_{\text{dec}}^2 + \Delta\omega_0^2)(\Gamma^2 + \Delta\omega_{\text{na}}^2) \\ &\quad + 2(\Gamma_{\text{dec}}\Gamma - \Delta\omega_0\Delta\omega_{\text{na}})\kappa^2 + \kappa^4, \end{aligned} \quad (14)$$

where $\Gamma_{\text{dec}} = \frac{1}{2}\Gamma_{\text{fs}} + \Gamma_{\text{d}}$ is the total decoherence rate of an atom, which includes contribution from spontaneous emission and pure dephasing processes. In the resonant

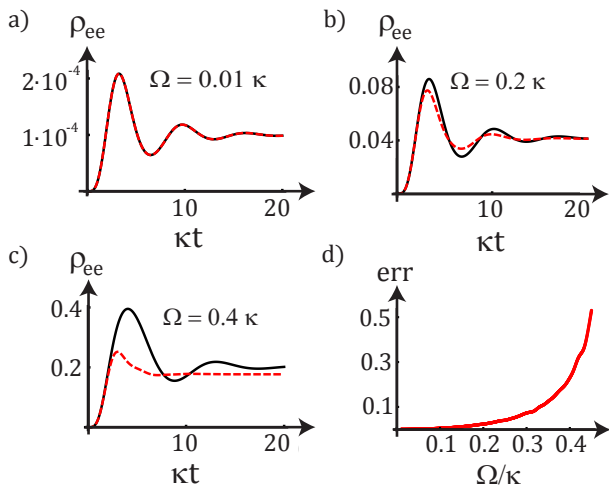


Fig. 2: Excited state occupation probability of the atom versus time, for $\omega_{\text{dr}} = \omega_{\text{na}} = \omega_0$, $\Gamma = 0.5\kappa$, $\Gamma_{\text{fs}} = 10^{-9}\kappa$, $\Gamma_{\text{d}} = 0$ and varying Rabi frequency of the driving field Ω . The black solid line corresponds to the semiclassical and the red dashed line to the fully quantum result. (a) In the case of weak driving fields, a perfect agreement is obtained. (b) & (c) For stronger driving fields, not only the time evolution, but also the steady state results are incorrectly evaluated in the semiclassical approximation (17). (d) The relative error of the steady-state results grows fast with the Ω/κ ratio.

case with $\omega_{\text{dr}} = \omega_{\text{na}} = \omega_0$, the validity criterion for the semiclassical approximation simplifies to

$$\rho_{ee}^{\text{sc}} \approx \frac{2\Gamma_{\text{dec}}}{\Gamma_{\text{fs}}} \frac{\kappa^2 \Omega^2}{(\Gamma_{\text{dec}}\Gamma + \kappa^2)^2} \ll 1. \quad (17)$$

This condition of weak driving fields is confirmed in numerical simulations.

We perform simulations assuming $\omega_{\text{dr}} = \omega_{\text{na}} = \omega_0$, $\Gamma = 0.5\kappa$, $\Gamma_{\text{fs}} = 10^{-9}\kappa$, $\Gamma_{\text{d}} = 0$, and varying the driving strengths. Initially, the atom is assumed to be in its ground state and the field amplitude of the nanoantenna vanishes: $\rho(t=0) = |g\rangle\langle g| \otimes |0\rangle\langle 0|$ is the initial condition for the fully quantum case, whereas $\rho^{\text{sc}}(t=0) = |g\rangle\langle g|$ and $\alpha(t=0) = 0$ corresponds to the semiclassical one. In the fully quantum approach we perform the calculations in a Hilbert space truncated at sufficiently high number k_{max} of excitations in the nanoantenna. Here it suffices to set $k_{\text{max}} = 10$. In Fig. 2, the excited state occupation probability of the atom is compared when calculated in the semiclassical (black solid line) and the fully quantum approach (red dashed line), for increasing intensities of the driving field [panels (a)-(c)]. For weak fields, and small excited state occupations, the results are in perfect agreement (a). Slightly stronger fields result in discrepancies in time evolution, but the steady state occupation is accordingly calculated in both approaches (b). This

is no longer the case for rather strong driving fields that result in considerable excitation probabilities of the atom (c). In panel (d) the steady-state relative error, defined as $\text{err} \equiv |\rho_{ee}^{\text{sc}} - \rho_{ee}| / \rho_{ee}|_{t \rightarrow \infty}$, is shown to grow fast with the ratio of the Rabi frequency of the driving field Ω to the coupling constant κ .

On more analytical grounds, we can first examine the simplest case where the spontaneous emission is the only source of decoherence, i.e. $\Gamma_{\text{d}} = 0$ and $\Gamma_{\text{dec}} = \frac{1}{2}\Gamma_{\text{fs}}$. Then, the prefactor in Eq. (17) is unity since $2\Gamma_{\text{dec}}/\Gamma_{\text{fs}} = 1$. Moreover, for small losses, Eq. (17) may be even further simplified. Then we find a condition for the validity of the semiclassical approach as $\Omega \ll \kappa$. If that condition holds $\rho_{ee}^{\text{sc}} \ll 1$, i.e., the atom shall approximately remain in its ground state. If losses dominate, i.e. for atoms weakly coupled to a nanoantenna, the semiclassical approximation can be applied as long as $\Omega \ll \Gamma\Gamma_{\text{fs}}/\kappa$.

When dephasing is additionally present ($\Gamma_{\text{d}} \neq 0$), the excited state occupation is always increased (not shown) with respect to the case of pure spontaneous emission, which makes condition (17) more difficult to be fulfilled. For small driving field intensities the peak value of the excited-state occupation probability is equal to $\rho_{ee}^{\text{sc}, \text{max}} \approx \Omega^2 / 2\Gamma_{\text{fs}}\Gamma$ and is reached for $\Gamma_{\text{dec}} = \kappa^2/\Gamma$. Thus we arrive at a strong worst-case-scenario criterion valid for an arbitrary dephasing rate and an arbitrary coupling strength: $\Omega^2 \ll \Gamma_{\text{fs}}\Gamma$.

This result may seem counterintuitive. One might have expected that the semiclassical approximation is valid in the limit of sufficiently strong rather than weak fields. This result can be understood as follows. For weak driving fields, in good approximation the atoms are in their ground states. Then, they behave as harmonic oscillators which can be accurately described by the semiclassical approach which is in line with the results presented in Ref. [17]. For stronger fields, the approximation of the two-level systems as harmonic oscillators breaks down and with it the semiclassical approach. However, for even stronger fields, the feedback of the atoms is not of considerable importance anymore. Mathematically, this interaction region can be defined by $|\alpha|^2 \gg 1$ which naturally leads to $\Omega \gg \Gamma$ and κ .

IV. DESIGN OF THE NANOANTENNA

In this section we aim at designing a nanoantenna that allows achieving the strong coupling regime. The latter can be defined as

$$\kappa > \Gamma. \quad (18)$$

This condition suggests that an excitation is exchanged between the atomic and the nanoantenna subsystems prior its eventual dissipation to the environment. (Here we treat the decay and decoherence rates in the atoms as

negligible in comparison with the losses by the nanoparticle.)

On our path to a design that allows for the strong coupling regime, we investigate how the coupling constants and loss rates can be tailored by varying shape and size of the nanoantenna. As a main result of this section we find that strong coupling can be achieved if the characteristic spatial dimensions of the nanoantenna, e.g. size as well as separation of elements forming the antenna, is in the order of 10 nm. Small spatial dimensions are eventually the crucial condition since they guarantee sufficiently small mode volumes as required to reach the strong coupling regime. In the following we analyze the nanoantennas in terms of two generic parameters that determine their radiative properties and are often at the focus of interest while engineering nanoantennas: the nanoantenna efficiency $\eta \equiv \Gamma_r/\Gamma$ and the Purcell factor F . The efficiency [26] is a measure for the fraction of radiative energy loss Γ_r by the nanoantenna when compared to its total energy loss $\Gamma = \Gamma_r + \Gamma_{nr}$. Here it is calculated for bare nanoantennas, i.e. at the absence of atoms. The Purcell factor is here understood as a measure for the nanoantenna's capability to enhance the radiation of a dipole source [9]. It naturally depends on the position of the source with respect to the nanoantenna. We find the Purcell factor by dividing the total energy flux calculated in the presence of the nanoantenna when compared to a situation where the nanoantenna is absent. The latter case corresponds to free-space emission rate Γ_{fs} . Note that it is a quantity different from what is usually called Purcell factor in the context of cavity QED, i.e. the enhancement of the decay rate of an atom [22, 26]. In the case of atoms interacting with a nanoantenna their decay rate can be enhanced due to both radiative and nonradiative loss channels of the nanoantenna. Only for nanoantennas of unitary efficiency the two quantities are equal. Our results prove that there is a trade-off between the nanoantenna efficiency or the Purcell factor, and the strength of the coupling that can be achieved with a nanoantenna.

In App. B, the methods that we use to compute the coupling constants and loss rates are described in detail for a specific nanoantenna. Our electromagnetic simulations were performed with COMSOL MULTIPHYSICS simulation platform where the dispersive permittivity has been fully considered [27]. The basic nanoantenna geometry which is considered from now on and obeys the assumptions made in the introduction is shown in Fig. 3(a). It consists of three identical silver nanospheroids with axis lengths a and b . For prolate nanospheroids $a > b$ holds. They are positioned at a distance r_0 from each other, along the x axis of the chosen coordinate system with its origin at the centre of the middle nanospheroid. Multiple nanospheroids are chosen because they have the potential to confine and enhance fields much stronger when compared to isolated nanospheroids. This leads to much larger coupling constants κ , being proportional

to the component of the enhanced field parallel to the transition dipole moment of the atom. We assume the latter to be the x direction.

To provide a visual impression of the spatial distribution of this enhanced field, we consider a design that turns out to provide the largest κ/Γ ratio: a nanoantenna made of prolate spheroids of $a = 13.3$ nm, $b = 8$ nm, and $r_0 = 2$ nm, subject to the driving field of frequency $\omega_{dr} = 3.37 \times 10^{15}$ Hz, which is the resonance frequency of the nanoantenna. (Note that when considering coupling to atomic systems, an exact resonance with the atomic transition frequency is not crucial, due to the broad plasmonic resonance.) The driving field propagates along the y direction and is polarized in x direction. We show in Fig. 3(b) the spatial distribution of the absolute value of the x -polarized component of the scattered field in the xy plane, normalized to the value of the incoming field. Only the scattered, not the total (scattered + driving) field is considered here, because the driving field is considerably weaker and its action on the atom can be neglected to a good approximation. This is in accordance with the assumptions made for the Hamiltonians given by expressions (1,6), considered in Sec. II.

For the following results, we scan the extinction cross-section of every nanoantenna, subject to a monochromatic driving field, in the frequency domain to find its plasmonic resonance frequency ω_{na} . We assume here a lossless host medium ($\epsilon = 2.2$). Next we consider a resonantly driven nanoantenna, to find both the loss rate Γ and the coupling constant κ at the point equidistant from the two spheroids, as described in App. B. We set the transition dipole moment of an atomic system to the rather high, but realistic value of $d_{ge} = 6 \times 10^{-29}$ Cm. We compare in Fig. 3(c) the κ/Γ ratio for nanoantennas of varying size (red circles) and aspect ratio (red crosses). The essential result is that the strong coupling regime may only be achieved for small nanoantennas (minor axis below 15 nm). Less important is the rather weak dependence on the aspect ratio a/b : the largest values of the κ/Γ ratio are obtained for prolate objects, as they are capable of confining and enhancing the fields stronger than oblate ones. In the same figure the dependence on the separation distance r_0 between the nanospheroids is displayed (blue squares). Also here the atoms are assumed to be situated exactly in-between the two nanospheroids, so increasing r_0 means also increasing the distance from the atom to the nanospheroids. This explains why the field enhancement, and with it the coupling constant κ , drops with the distance r_0 . Strong field enhancements, and thus strong couplings, are obtained if the nanospheroids are less than 4 nm apart from each other.

Let us now analyze the efficiencies of the above-considered nanoantennas [see Fig. 3(d)]. According to our investigations, a small size, which is the key for strong coupling, will result in poor nanoantenna efficiencies.

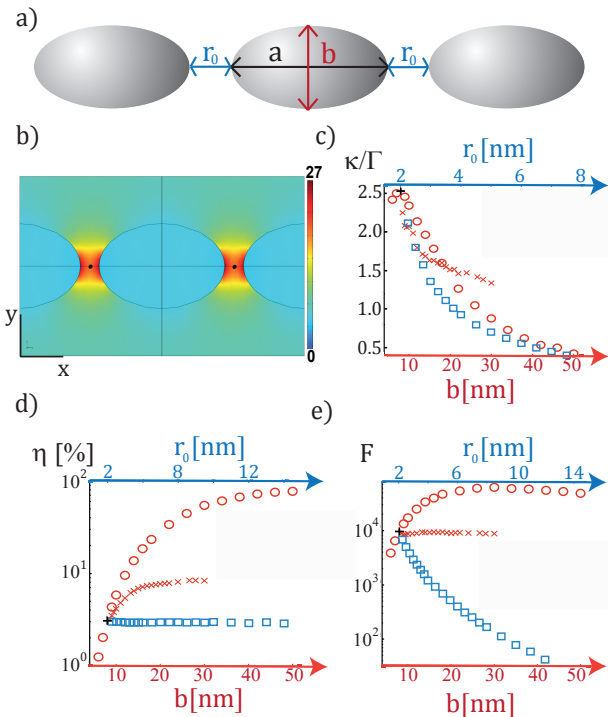


Fig. 3: (a) General scheme of the nanoantenna consisting of three identical nanospheroids of aspect ratio a/b , positioned at distance r_0 from each other. (b) Distribution of the absolute value of the x -polarized component of the scattered field (normalized by the value of the incoming field) for three identical nanospheroids with $a = 13.3$ nm and $b = 8$ nm and separated by $r_0 = 2$ nm. The coupling constant κ is proportional to the enhancement of the x -polarized scattered field component at the point where the atom is placed. (c) κ/Γ ratio for $d_{ge} = 6 \times 10^{-29}$ Cm and various geometrical parameters of the nanoantenna: dependence on size for a fixed distance (red circles, constant aspect ratio $a/b = 1.67$, $r_0 = 2$ nm), on aspect ratio for a fixed distance (red crosses, constant $a = 13.3$ nm, $r_0 = 2$ nm), and on distance r_0 for fixed size of the nanospheroids (blue squares, $a = 13.3$ nm and $b = 8$ nm). The value of κ is always calculated at the point equidistant from the tips of the nanospheroids [black colored dot in (b)]. (d) Nanoantenna efficiency and (e) Purcell factor, values of parameters as in (c). The particular design that corresponds to the largest κ/Γ ratio and the scattered field distribution of panel (b), is described in the text and marked in (c)-(e) with the black cross.

The efficiency reaches up to 54% for nanospheroids with a minor axis of 30 nm and drops dramatically as the size decreases. In Ref. [28] such scaling of the size-dependent efficiency has been rigorously derived for spherical particles in terms of scattering and absorption cross sections. Also for prolate objects the efficiency drops. The impact of particular nanospheroids on each other's radiative losses and absorption turns out to be marginal, so the efficiencies of the proposed nanoantennas shows little dependence on the distance between the nanospheroids.

Relatively higher radiative losses in large nanoantennas

result in an increase of the Purcell factor [see Fig. 3(d)]. Again, it is the size that determines to a large extent the radiative losses of the nanoparticle. This is why the Purcell factor is almost constant for varying aspect ratio, for the size of the nanoantenna is here almost fixed. Naturally, the Purcell factor decreases fast as the distance between the nanoantenna and the dipole source grows, since then the interplay between them becomes significantly less intense.

Out of the geometries considered above, the optimum for strong coupling (i.e. the one that provides the largest κ/Γ ratio) is always marked with the black cross. Its explicit geometrical parameters are the same as those used for plotting Fig. 3(b). For such design, we obtain $\Gamma_{nr} = 7.0 \times 10^{13}$ Hz, $\Gamma_r = 6.0 \times 10^{12}$ Hz. (Once again, we note that small nanoantennas designed for strong coupling turn out to be rather poor emitters: nonradiative losses overcome radiative losses by more than an order of magnitude.) The coupling constant with each of the atoms amounts to $\kappa = 2.3 \times 10^{14}$ Hz. Its large value is responsible for the vivid dynamics of the hybrid system subject to the driving field, and for multiple exchange of excitations before their dissipation into the environment by the nanoantenna.

An example of such behaviour is presented in Fig. 4, with the calculations performed in the fully quantum approach with the Hilbert space truncated at $k_{max} = 10$. The hybrid system is initially in its ground state. It is subject to a driving field of Rabi frequency $\Omega = 0.5\kappa$ which quickly leads to an increase of the probability of a single photon excitation of the nanoantenna, followed by the probability of a single symmetric excitation in the atomic subsystem: in the figure, the occupation probability of the state $|S\rangle = (|e^{(1)}\rangle|g^{(2)}\rangle + |g^{(1)}\rangle|e^{(2)}\rangle) / \sqrt{2}$ is shown. Next, also the probability of double excitations rises. At the driving field intensities as small as the one applied here, higher-order excitations in the nanoantenna are negligible. After exchanging the excitations several times between the atomic and nanoantenna subsystems, the hybrid system finally relaxes to a steady state, where equilibrium is reached by the driving field and the losses. Note that this result, with a significant probability of symmetric state occupation, suggests considerable entangling power of nanoantennas, which has been explored e.g. in Refs. [29, 30].

The results of this section prove that while engineering a nanoantenna one has to keep in mind the trade-off between the strength of the coupling that can be achieved with a particular design, and the corresponding efficiency and ability of the nanoantenna to enhance radiation of dipole emitters. The size of the structure turns out to be the key parameter, which needs to be small for achieving the strong coupling regime. Then, the hybrid system undergoes a complicated dynamics. It is also interesting to analyze its spectral properties, which is at the focus of the following section. For any deviating condition as consid-

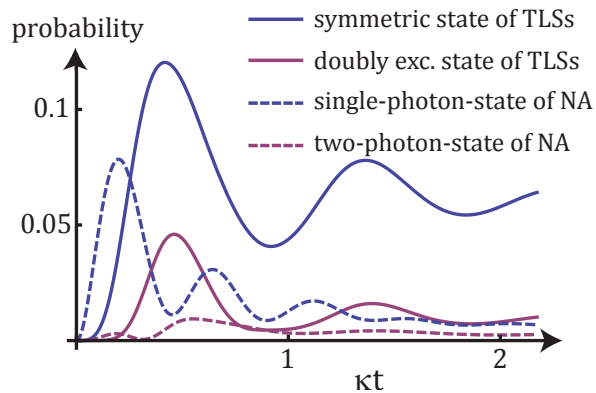


Fig. 4: Strong coupling between the atomic systems and the nanoantenna is manifested in the dynamics by the mutual exchange of excitations (atomic - solid lines, nanoantenna - dashed lines). Peaks in occupation probabilities of the symmetric (blue solid line, results multiplied by a factor of 0.5) and doubly excited (purple solid line) states, correspond to dips in probabilities of presence of one (blue dashed line) and two (purple dashed line) photons in the system. Nanoantenna and atomic parameters described in the text.

ered further below, a suitable nanoantenna that correctly reflects the situation as considered can be identified out of the data presented in this section. Figure 3 can serve here as guideline, from which a possible geometry can be derived for a realization of a given κ/Γ rate.

V. MODIFICATION OF SPECTRA

In this section we study how the presence of two atoms coupled to a nanoantenna modifies its extinction spectrum. Such modification is profound in the strong coupling regime and at the single-quantum level of excitation. We compare the results with the single atom case to prove the sensitivity of the hybrid quantum system to the number of atomic systems involved.

The combined system permits several loss channels: the radiative and non-radiative losses of the nanoantenna and the spontaneous emission and dephasing in the atoms. In the studied scenario, the nanoantenna is strongly coupled to the two atoms. Hence, one may assume that any emission by an atom is absorbed by the nanoantenna [31]. Thus, the loss of the nanoantenna can be used as a figure of merit to understand the loss of the combined system. The total extinct (absorbed and scattered) power is given by $P(\omega_{\text{dr}}) \equiv \hbar\omega_{\text{na}}\Gamma\langle a^\dagger a \rangle$. It is a quantity directly accessible in a possible experiment. Here, $\langle a^\dagger a \rangle = \text{Tr}[a^\dagger a \rho(t \rightarrow \infty)]$ denotes the mean number of photons in the system's steady state $\rho(t \rightarrow \infty)$. Note that because of the rather low efficiency of the nanoantenna, i.e. $\Gamma_{\text{nr}} \gg \Gamma_{\text{r}}$, the extinction spec-

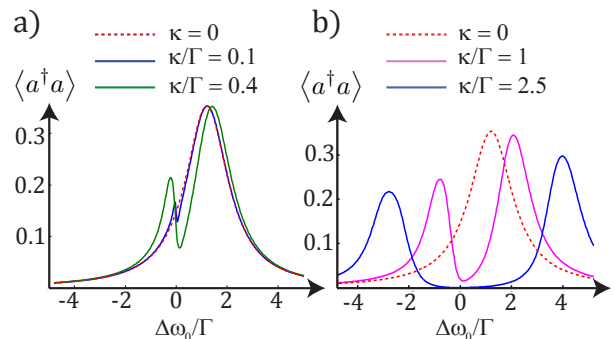


Fig. 5: Impact of atoms on the extinction spectra of the combined system for different coupling strengths κ in the weak (a) and strong coupling regime (b). Steady-state mean number of photons is plotted versus the driving-field detuning from atomic transition frequency $\Delta\omega_0$. The red dashed line corresponds to no coupling, i.e. the bare nanoantenna. A Fano-like behavior can be observed for increased but still weak coupling. The results have been obtained for weak driving fields of Rabi frequencies $\Omega = 0.6\Gamma$. Furthermore, a rather small detuning between nanoantenna and atoms $\omega_{\text{na}} - \omega_0 = 1.2\Gamma$ is assumed. The blue line in panel (b) corresponds to the antenna design of Sec. IV.

trum is dominated by the absorption spectrum.

Even though the losses are almost entirely due to the nanoantenna, the extinction spectrum may be strongly influenced by the two atoms. This is especially the case when the driving field is weak and the hybrid system remains at the single-excitation level. This strength of the contribution of the atoms to the overall spectrum naturally depends significantly on the coupling as it is illustrated in Fig. 5. For weak couplings [see panel (a)], a broad plasmonic resonance dominates the extinction spectrum and a perturbation at the transition frequency of the atoms can be observed. For strong couplings [panel (b)], the plasmonic and atomic contributions to the spectrum can no longer be distinguished. Extinction at atomic transition frequency is significantly reduced and Rabi peaks are visible at the sides. It is interesting to note that the extinction peaks can be spectrally shifted much further when compared to the linewidth due to the strong coupling. The latter is thus a crucial condition for a strong impact of the atoms on the extinction spectrum of a nanoantenna.

Generally, the spectrum can be understood in terms of a hybridization caused by the interaction of all subsystems. The eigenstates and eigenenergies can be derived according to the Jaynes-Cummings model which is outlined in App. C in detail. The latter are plotted in Fig. 6 for both cases of a single and two atoms coupled to a nanoantenna. In the resonant case of $\omega_{\text{na}} = \omega_0$ the splitting between the first pair of excited states is equal

to $\sqrt{N_{\text{tIs}}}\kappa$. This simple example proves that the spectrum of the hybrid system, i.e. the position of the Rabi peaks, crucially depends on the number of atoms. Furthermore, the effective increasing of the coupling constant by the factor of $\sqrt{N_{\text{tIs}}}$ may help to overcome losses and fulfill the strong coupling condition (18).

The analysis of the diagrams in Fig. 6 suggests that, in principle, one might expect an even stronger manifestation of the number of atoms in the spectra for slightly more intense driving fields, where highly-excited states ($n \geq 2$) become occupied. For this purpose, however, couplings even stronger than those obtained with the design of Sec. IV would be preferable. Otherwise, the required sensitivity to trace the contribution of highly excited states to the spectra may not be reached due to significant nanoantenna losses.

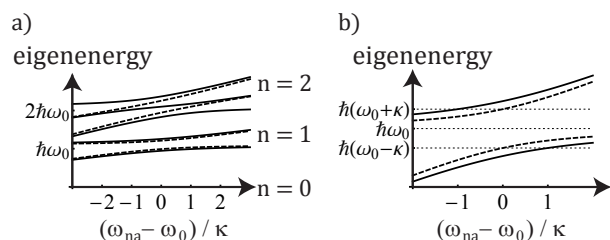


Fig. 6: (a) Eigenenergies of the hybrid system as functions of the detuning between nanoantenna resonance frequency and atomic transition frequency for the case of $N_{\text{tIs}} = 1$ (dashed lines) and $N_{\text{tIs}} = 2$ (solid lines). Only energies of states corresponding to the total number of excitations $n \leq 2$ are shown. (b) Zoomed view for $n = 1$. Energy splitting of the first pair of excited states compared for the cases $N_{\text{tIs}} = 1$ and $N_{\text{tIs}} = 2$. In the latter case it is larger by a factor of $\sqrt{2}$ for $\omega_{\text{na}} = \omega_0$.

The interesting question arises whether the influence of the atoms on the extinction spectra remains so significant for stronger driving fields, i.e. beyond the quantum regime. To investigate such transition we performed calculations for increasing driving intensities for the case of strong coupling proposed in Section IV. The results are displayed in Fig. 7(a). For weak driving fields (blue line) a splitting can be observed with Rabi peaks at $\Delta\omega_0 = \pm\sqrt{2}\kappa$, as well as an onset of transparency at $\Delta\omega_0 = 0$, as measured in cavity QED systems, see Refs. [32, 33]. As the strength of the driving field grows, the corresponding extinction peaks are shifted towards the center. Finally, in the limit of strong driving field defined as $\Omega > \Gamma$, the contribution from the atomic systems becomes negligible and the bare nanoantenna spectrum is recovered.

To understand this behaviour, we analyze the occupation probabilities of the hybrid system's eigenstates. In the case of weak driving fields, only the first pair of excited eigenstates $|\psi_{1,\pm}\rangle$, of energies equal to $\hbar\omega_0 \pm \hbar\sqrt{2}\kappa$,

is populated. The occupation probabilities of states $|\psi_{1,+}\rangle$ and $|\psi_{2,+}\rangle$ for such case are plotted in Fig. 7(b) and it can be seen that for the latter state it is indeed negligible. The occupation probabilities of states $|\psi_{1,-}\rangle$ and $|\psi_{2,-}\rangle$ (not shown) are peaks symmetric with respect to $|\psi_{1,+}\rangle$ and $|\psi_{2,+}\rangle$, i.e. they are centred at $\omega = \omega_0 + \sqrt{2}\kappa$. For an increased driving field, the probability of exciting higher-energy states becomes significant [see green lines in Fig. 7(b)]. It is the reason for shifting the Rabi peaks towards the centre. As the driving field rises, the energy difference between subsequent occupied eigenstates tends to ω_{na} , which explains why in the strong driving field limit $\Omega > \Gamma$ the result corresponds to the bare nanoantenna case. This statement can be also derived from the steady-state solution of the Heisenberg equations of motion where one finds that $\langle a^\dagger a \rangle \approx \Omega^2/\Gamma^2 \gg N_{\text{tIs}}$ should hold. This means that indeed for stronger driving fields we rediscover the classical behaviour of the nanoantenna, irrespective of the presence of the atoms.

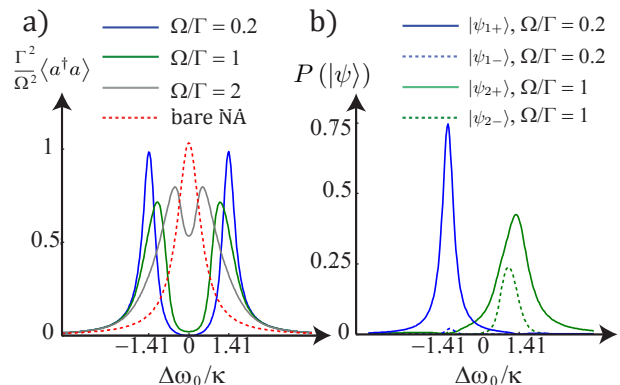


Fig. 7: (a) Impact of the driving field intensity on extinction spectra, normalized by a dimensionless parameter Γ^2/Ω^2 , for the strong coupling nanoantenna proposed in Sec. IV. (b) Probability of occupation of the first ($n = 1$, solid lines) and second ($n = 2$, dashed lines) pair of excited states $|\psi_{n,\pm}\rangle$ for the cases of driving field Rabi frequencies $\Omega = 0.2\Gamma$ (blue lines, results multiplied by a factor of 10) and $\Omega = \Gamma$ (green lines).

VI. CONCLUSIONS

In this paper, we have investigated the coupling of one and two atoms approximated by two-level systems to optical nanoantennas. It was outlined that the use of a fully quantum approach to understand the dynamics of the system is necessary. Only for extremely weak driving fields a semiclassical formulation of the nanoantenna dynamics may be used.

At the design stage of a nanoantenna a trade-off must be achieved between the field enhancement by the

nanoantenna, directly responsible for the strength of the coupling, and the nanoantenna's efficiency. Small size, which results in high absorption losses, is essential for achieving the strong coupling regime. Then, the spectra of the combined system are hugely influenced by the presence of the atoms if only the driving field is considerably weak, i.e. in the quantum regime.

Furthermore we have shown that a strong coupling of several atoms to a nanoantenna does change the spectrum significantly. Such features will enable experimentalists to identify situations of multiple coupled atoms in the strong coupling regime.

Acknowledgement

This work was partially supported by the German Federal Ministry of Education and Research (PhoNa) and by the Thuringian State Government (MeMa).

Appendix A: Classical field dynamics

In this section we will outline semiclassical treatment of the nanoantenna used in this paper. Especially, we will derive the equations of motion for the respective electric field in dependence on the state of the atoms.

If a plasmonic structure like the discussed nanoantenna is much smaller than the wavelength, it can be understood as a classical harmonic oscillator as it is long known in the metamaterials community, see e.g. Ref. [34]. The scattered field $\tilde{\mathbf{E}}_{\text{sca}}(\mathbf{r}, t)$ of such an oscillator may be separated into a temporally and spatially varying one and a spatial term:

$$\tilde{\mathbf{E}}_{\text{sca}}(\mathbf{r}, t) = \tilde{\alpha}(t) \mathbf{E}_{\text{sca}}(\mathbf{r}) + \text{c.c.} \quad (\text{A1})$$

The spatial part $\mathbf{E}_{\text{sca}}(\mathbf{r})$ can be found by computer simulations or analytical considerations. We assume that this spatial component, which may also be denoted as mode profile, does not change for the excitations we discuss in the following. Then, the whole nanoantenna dynamics is exclusively described by the evolution of the temporal part $\tilde{\alpha}(t)$ for which the equations of motion will be derived and solved in the following.

Under the assumption of an oscillator-like evolution, the positive frequency part $\tilde{\alpha}(t)$ evolves according to the equation

$$\ddot{\tilde{\alpha}}(t) + \Gamma \dot{\tilde{\alpha}}(t) + \omega_{\text{na}}^2 \tilde{\alpha}(t) = F(t) e^{-i\omega_{\text{dr}} t}, \quad (\text{A2})$$

where $F(t) e^{-i\omega_{\text{dr}} t}$ corresponds to the driving field at the nanoantenna site. In our case it is proportional to the driving laser field and the assumed dipolar fields of the two atoms.

We assume the driving term to oscillate at a mean frequency ω_{dr} . Then, its envelope $F(t)$ shall vary much

slower. Consequentially, we can also calculate the solutions to the equations of motion for a slowly-varying part of the nanoantennas oscillation defined via $\tilde{\alpha}(t) = \alpha(t) e^{-i\omega_{\text{dr}} t}$. Then in the standard slowly-varying envelope approximation ($|\dot{\alpha}| \ll |\alpha \omega_{\text{dr}}|$) and accounting for $\Gamma \ll \omega_{\text{dr}}$ one arrives at the equations of motion for the electric field of the nanoantenna as

$$\dot{\alpha}(t) = -\Gamma \alpha(t) + \frac{i}{2\omega_{\text{dr}}} [(\omega_{\text{dr}}^2 - \omega_{\text{na}}^2) \alpha(t) + F(t)]. \quad (\text{A3})$$

For near-resonance driving fields ($\omega_{\text{na}}^2 - \omega_{\text{dr}}^2 \approx 2\omega_{\text{dr}} \Delta\omega_{\text{na}}$), the above equation further reduces to:

$$\dot{\alpha}(t) = -(\Gamma + i\Delta\omega_{\text{na}}) \alpha(t) + iF(t)/2\omega_{\text{dr}}, \quad (\text{A4})$$

We now compare equation (A4) with the Heisenberg operator equation in the fully quantum approach, $\dot{a}(t) = -(\Gamma + i\Delta\omega_{\text{na}}) a(t) + i[\kappa \sum_j \sigma_-^{(j)}(t) + \Omega] + f(t)$, where $f(t)$ stands for the Langevin noise operator such that $\langle f(t) \rangle = 0$ [22], which originates from coupling of the field of the nanoantenna with its electromagnetic environment and with phonons. With such a direct comparison, we can identify the driving term

$$F(t) = 2\omega_{\text{dr}} \left[\kappa \sum_j \rho_{eg}^{\text{sc}(j)}(t) + \Omega \right], \text{ so} \quad (\text{A5})$$

$$\begin{aligned} \dot{\alpha}(t) = & -(\Gamma + i\Delta\omega_{\text{na}}) \alpha(t) \\ & + i \left[\kappa \sum_j \rho_{eg}^{\text{sc}(j)}(t) + \Omega \right]. \end{aligned} \quad (\text{A6})$$

With the latter equation, we arrived at the evolution equation for the electric field of the nanoantenna in the semiclassical picture. Our result corresponds to the equation of motion of the mean value of quantum operators, with the nanoantenna's field approximated by a coherent state $|\alpha(t)\rangle$.

Appendix B: Calculation of parameters

In Appendix A we have derived the equations of motion for electric field of a nanoantenna coupled to an unspecified number of noninteracting atoms. Now we will specify how to obtain the relevant system parameters from electromagnetic simulations. The key for determining the coupling constants and loss rates lies in the determination of the nanoantenna field for a single excitation as we will see shortly.

**Coupling constant between
nanoantenna and atoms: κ**

In electric dipole approximation the constant describing the coupling strength between the j 'th atom and the nanoantenna is given by

$$\kappa_j = \mathbf{E}_{\text{sca}}^{\text{se}}(\mathbf{r}_j) \cdot \mathbf{d}_{ge}^{(j)} / \hbar, \quad (\text{B1})$$

where $\mathbf{d}_{ge}^{(j)}$ stands for the transition dipole moment element in the j 'th atom. In the considered case the atoms are assumed to be identical, so the index j can be dropped. Naturally, here the field $\mathbf{E}_{\text{sca}}^{\text{se}}$ corresponds to a single excitation of the nanoantenna taken at the position of any of the atoms. Because of their symmetric positioning and the mirror symmetry of the nanoantenna, $\mathbf{E}_{\text{sca}}^{\text{se}}(\mathbf{r}_1) = \mathbf{E}_{\text{sca}}^{\text{se}}(\mathbf{r}_2)$ holds which would prevent excitation of the antisymmetric state of the atomic subsystem for the lossless case, see App. C. So, κ depends on the dipole moment of both atoms, the scattered field of the nanoantenna and the very location of the atoms.

To find the correct scaling for κ , the electric field has to be calculated at the positions of the atoms for an excitation of the nanoantenna due to a single photon with energy $\hbar\omega_{\text{na}}$. Thus, for a computation at the nanoantenna's resonance, first the field energy for the corresponding excited electromagnetic mode $\mathbf{E}_{\text{sca}}(\mathbf{r})$ has to be determined using the well-known energy-density integration for dispersive media [35]

$$W = \frac{1}{2} \int \frac{\partial}{\partial \omega} [\omega \Re \varepsilon(\omega)] \Big|_{\omega=\omega_{\text{na}}} |E_{\text{sca}}(\mathbf{r})|^2 dV \quad (\text{B2}) \\ + \frac{1}{2} \int \mu_0 |H_{\text{sca}}(\mathbf{r})|^2 dV.$$

Then, the electric field of a single-photon excitation is given by

$$\mathbf{E}_{\text{sca}}^{\text{se}}(\mathbf{r}) = \sqrt{\hbar\omega_{\text{na}}/W} \mathbf{E}_{\text{sca}}(\mathbf{r}), \quad (\text{B3})$$

since the energy of the nanoantenna's mode corresponds to $N = W/\hbar\omega_{\text{na}}$ photons.

**Coupling constant between nanoantenna and driving
field: Rabi frequency Ω**

The Rabi frequency Ω describes the coupling of the nanoantenna and the driving field. It can be evaluated in the dipole approximation as $\Omega = \mathbf{d}_{\text{na}}^{\text{se}} \cdot \mathbf{E}_{\text{dr}} / \hbar$, where $\mathbf{d}_{\text{na}}^{\text{se}}$ is the dipole moment of the nanoantenna corresponding to a single excitation for which the electric field is known from the previous subsection. The dipole moment $\mathbf{d}_{\text{na}}^{\text{se}}$ can then just be calculated from a multipole expansion of $\mathbf{E}_{\text{sca}}^{\text{se}}(\mathbf{r})$. For our calculations, the main contribution to the far-field of the nanoantenna was indeed that from the dipole moment which justifies the calculation of Ω in the dipole approximation.

**Radiative and nonradiative losses
of the nanoantenna: Γ**

The losses of the nanoantenna can be divided into radiative and non-radiative losses, $\Gamma = \Gamma_{\text{r}} + \Gamma_{\text{nr}}$. Both quantities are related to integrations of the nanoantenna mode for a single excitation $\mathbf{E}_{\text{sca}}^{\text{se}}(\mathbf{r})$: The radiative loss Γ_{r} can be determined by the integral over the time-averaged Poynting vector over a closed surface embedding the nanoantenna, $\Gamma_{\text{r}} = \int \langle \mathbf{S}_{\text{sca}}^{\text{se}}(\mathbf{r}, t) \rangle d\mathbf{A}$. The non-radiative part is given by a volume integral over the nanoantenna using Ohm's law, $\Gamma_{\text{nr}} = \int \sigma \langle \mathbf{E}_{\text{sca}}^{\text{se}}(\mathbf{r}, t) \rangle^2 dV$, where σ is the electric conductivity of the metal.

Appendix C: Eigenstates of the free Hamiltonian

Here we will analyze the Hamiltonian of the nanoantenna coupled to two two-level systems in the fully quantum case. As one might expect, we will arrive at a simple generalization of the Jaynes-Cummings model and give the energy spectrum of its eigenstates.

It is often advantageous to analyze problems of coupled two-level systems in the so-called Dicke basis that relates ground and excited states, $|g\rangle$ and $|e\rangle$, of each two-level system to a combined eigenbasis [36]: $\{|D\rangle \equiv |e\rangle \otimes |e\rangle, |S\rangle \equiv \frac{1}{\sqrt{2}}(|e\rangle \otimes |g\rangle + |g\rangle \otimes |e\rangle), |A\rangle \equiv \frac{1}{\sqrt{2}}(-|e\rangle \otimes |g\rangle + |g\rangle \otimes |e\rangle), |G\rangle \equiv |g\rangle \otimes |g\rangle\}$, with the doubly excited state $|D\rangle$, the symmetric and antisymmetric states $|S\rangle$ and $|A\rangle$ with a single excitation, and the ground state $|G\rangle$. In the Dicke basis, the Hamiltonian reads as

$$H = \frac{1}{2} \hbar\omega_0 (2|D\rangle\langle D| + |S\rangle\langle S| + |A\rangle\langle A|) + \hbar\omega_{\text{na}} a^\dagger a \\ - \hbar\sqrt{2}\kappa (\Sigma_+ a + a^\dagger \Sigma_-), \quad (\text{C1})$$

where

$$\Sigma_+ = \frac{1}{\sqrt{2}} (\sigma_+^{(1)} + \sigma_+^{(2)}) = |D\rangle\langle S| + |S\rangle\langle G| \text{ and} \\ \Sigma_- = \Sigma_+^\dagger,$$

are the creation and annihilation operators of the atomic subsystem. Note that the antisymmetric state is decoupled in the isolated system and can be populated only by decay mechanisms or by an asymmetric drive. From now on it suffices to consider only the effective three-level system, whose state belongs to the Hilbert space spanned by $\{|G\rangle, |S\rangle, |D\rangle\}$.

We will give the explicit form of the eigenstates of the Hamiltonian and the corresponding eigenenergies in the case of resonance between the atomic and plasmonic systems, i.e. when $\omega_{\text{na}} = \omega_0$. The states of the hybrid system can be expressed in the Dicke basis for the atomic subsystem, and Fock basis $\{|k\rangle\}_{k=0}^\infty$ for the nanoantenna, with k denoting the number of photons in the system.

Each state can be characterized by the total number of excitations n it corresponds to. For instance, $n = 0$ stands for the total ground state of the system $|\psi_0\rangle = |G, 0\rangle$ of energy $E_0 = 0$. For a single excitation $n = 1$ we have two eigenstates and eigenvalues:

$$|\psi_{1,\pm}\rangle = \pm|S, 0\rangle + |G, 1\rangle, \quad (\text{C2})$$

$$E_{1,\pm} = \hbar\omega_0 \mp \sqrt{2}\hbar\kappa. \quad (\text{C3})$$

For the numbers of excitations $n \geq 2$ there are three eigenstates for a given n :

$$|\psi_{n,\pm}\rangle = \sqrt{n-1}|D, n-2\rangle \pm \sqrt{2n-1}|S, n-1\rangle + \sqrt{n}|G, n\rangle, \quad (\text{C4})$$

$$E_{n,\pm} = n\hbar\omega_0 \mp \sqrt{2(2n-1)}\hbar\kappa, \quad (\text{C5})$$

$$|\psi_{n,0}\rangle = \sqrt{n}|D, n-2\rangle - \sqrt{n-1}|G, n\rangle, \quad (\text{C6})$$

$$E_{n,0} = n\hbar\omega_0. \quad (\text{C7})$$

For visibility, the states are not normalized. Note that the eigenstates of the total system cannot be written as a product of states of atomic and nanoantenna subsystems. This is a clear sign of strong interaction of the subsystems that leads to their entanglement. The latter is a solely quantum feature which cannot be accounted for with the semiclassical formalism. Our condition for validity of the semiclassical approach can now be seen from a different perspective: the semiclassical description can be applied only if entanglement is present in the system with negligible probability.

The eigenstates obey a more complicated form, if the two-level systems are not in resonance with the nanoantenna ($\omega_{\text{na}} \neq \omega_0$). Then, the energy diagram depends strongly on the detuning, see again Fig. 6. In the strongly off-resonant limit, the interaction becomes negligible and the atomic and the nanoantenna subsystems behave independently. Consequentially, the eigenenergies tend to the unperturbed values.

For large numbers of excitations, the eigenstates become approximately separable:

$$|\psi_{n,\pm}\rangle \approx \left(|D\rangle \pm \sqrt{2}|S\rangle + |G\rangle\right) \otimes |n\rangle, \quad (\text{C8})$$

$$|\psi_{n,0}\rangle \approx (|D\rangle - |G\rangle) \otimes |n\rangle, \quad (\text{C9})$$

with the interaction energies: $\Delta E_{n,\pm} = \mp 2\hbar\kappa\sqrt{n}$, $\Delta E_{n,0} = 0$. This means, that in the limit of large field intensities, even though the field has strong influence on the atoms, the atoms approximately do not affect the field and the semiclassical approach can be applied again.

-
- [1] P. Anger, P. Bharadwaj, and L. Novotny, Phys. Rev. Lett. **96**, 113002 (2006).
 [2] A. G. Curto, G. Volpe, T. H. Taminiau, M. P. Kreuzer, R. Quidant, and N. F. van Hulst, Science **329**, 930 (2010).

- [3] X. Zhu, F. Xie, L. Shi, X. Liu, N. A. Mortensen, S. Xiao, J. Zi, and W. Choy, Opt. Lett. **37**, 2037 (2012).
 [4] A. Mohtashami and A. F. Koenderink, New J. Phys. **15**, 043017 (2013).
 [5] L. Novotny and N. van Hulst, Nat. Phot. **5**, 83 (2011).
 [6] L. Rogobete, F. Kaminski, M. Agio, and V. Sandoghdar, Opt. Lett. **32**, 1623 (2007).
 [7] J. Kern, S. Grossmann, N. V. Tarakina, T. Häckel, M. Emmerling, M. Kamp, J.-S. Huang, P. Biagioni, J. C. Prangsma, and B. Hecht, Nano Lett. **12**, 5504 (2012).
 [8] A. M. Kern and O. J. F. Martin, Phys. Rev. A **85**, 022501 (2012).
 [9] R. Filter, S. Mühlig, T. Eichelkraut, C. Rockstuhl, and F. Lederer, Phys. Rev. B **86**, 035404 (2012).
 [10] G. JP Reithmaier, A. Löffler, C. Hofmann, S. Kuhn, S. Reitzenstein, L. Keldysh, V. Kulakovskii, and A. TL Reinecke, Nature **432**, 197 (2004).
 [11] T. Aoki, B. Dayan, E. Wilcut, W. Bowen, A. Parkins, T. Kippenberg, K. Vahala, and H. Kimble, Nature **443**, 671 (2006).
 [12] J. Yan, W. Zhang, S. Duan, X. Zhao, and A. Govorov, Physical Review B **77**, 165301 (2008).
 [13] R. Artuso, G. Bryant, A. Garcia-Etxarri, and J. Aizpurua, Phys. Rev. B **83**, 235406 (2011).
 [14] J. Zuloaga, E. Prodan, and P. Nordlander, ACS Nano **4**, 5269 (2010).
 [15] A. Manjavacas, F. Abajo, and P. Nordlander, Nano Lett. **11**, 2318 (2011).
 [16] A. Trügler and U. Hohenester, Phys. Rev. B **77**, 115403 (2008).
 [17] E. Waks and D. Sridharan, Phys. Rev. A **82**, 043845 (2010).
 [18] D. Dzsojtjan, J. Kästel, and M. Fleischhauer, Phys. Rev. B **84**, 075419 (2011).
 [19] W. Zhang and A. O. Govorov, Phys. Rev. B **84**, 081405 (2011).
 [20] T. Hümmer, F. J. Garcia-Vidal, L. Martin-Moreno, and D. Zueco, Phys. Rev. B **87**, 115419 (2013).
 [21] J. Wolters, G. Kewes, A. W. Schell, N. Nüsse, M. Schoengen, B. Löchel, T. Hanke, R. Bratschitsch, A. Leitenstorfer, T. Aichele, et al., Phys. Status Solidi B **249**, 918 (2012).
 [22] P. Meystre and M. Sargent, *Elements of Quantum Optics* (Springer Verlag, 1999).
 [23] D. Heiss, S. Schaeck, H. Huebl, M. Bichler, G. Abstreiter, J. Finley, D. Bulaev, and D. Loss, Phys. Rev. B **76**, 241306 (2007).
 [24] X.-W. Chen, V. Sandoghdar, and M. Agio, Phys. Rev. Lett. **110**, 153605 (2013).
 [25] U. Dorner and P. Zoller, Phys. Rev. A **66**, 023816 (2002).
 [26] B. H. L. Novotny, *Principles Of Nano-Optics* (Cambridge University Press, 2006), ISBN 9780521149037.
 [27] E. Palik, *Handbook of Optical Constants of Solids*, no. Bd. 1 in Handbook of Optical Constants of Solids, Five-Volume Set (Elsevier Science, 1985), ISBN 9780080547213.
 [28] C. Bohren and D. R. Huffman, *Absorption and Scattering of Light by Small Particles* (Wiley Science Paperback Series, 1998).
 [29] A. Gonzalez-Tudela, D. Martin-Cano, E. Moreno, L. Martin-Moreno, C. Tejedor, and F. J. Garcia-Vidal, Phys. Rev. Lett. **106**, 020501 (2011).
 [30] D. Martin-Cano, A. Gonzalez-Tudela, L. Martin-Moreno, F. J. Garcia-Vidal, C. Tejedor, and E. Moreno, Phys.

- Rev. B **84**, 235306 (2011).
- [31] D. E. Chang, A. S. Sørensen, P. R. Hemmer, and M. D. Lukin, Phys. Rev. Lett. **97**, 053002 (2006).
- [32] C. Hood, M. Chapman, T. Lynn, and H. Kimble, Phys. Rev. Lett. **80**, 4157 (1998).
- [33] R. Miller, T. Northup, K. Birnbaum, A. Boca, A. Boozer, and H. Kimble, Journal of Physics B: Atomic, Molecular and Optical Physics **38**, S551 (2005).
- [34] J. Petschulat, C. Menzel, A. Chipouline, C. Rockstuhl, A. Tuennermann, F. Lederer, and T. Pertsch, Phys. Rev. A **78**, 043811 (2008).
- [35] L. Landau and E. Lifschitz (1984).
- [36] R. Dicke, Phys. Rev. **93**, 99 (1954).